Double Gimballed Reaction Wheel Maneuvering and Attitude Control System

E. D. Scott* and J.E. Rubbo†
Lockheed Missiles and Space Company, Inc., Sunnyvale, Calif.

A controller capable of precise large-angle open-loop maneuvering of a vehicle in roll and/or pitch, and of providing three-axis stabilization about the vehicle's maneuvered attitude is described. The controller commands a momentum biased double gimballed reaction wheel, and needs only roll and pitch horizon sensor information. No direct yaw sensor is used. The controller, a digital processor simulating a model of the vehicle/wheel system, is switched to either the maneuvering or attitude-hold made by a simple change of controller inputs. The controller is capable of performing maneuvers without exciting the long time constant yaw axis. Serial maneuvers may be performed without any intervening settling time. In the attitude-hold mode the controller significantly reduces gyroscopic coupling between axes, except for yaw into roll, and roll/yaw perturbations caused by orbit motion are eliminated. Yaw attitude is passively controlled by the gyroscopic wheel stiffness, and is actively damped by feeding a fraction of the roll activated control torque into yaw. The fraction varies as a function of the vehicle attitude and the wheel momenta to maintain a constant yaw damping ratio. Linear analysis and nonlinear simulation results are presented which demonstrate the controller's capabilities.

Nomenclature

Ax = the cross product matrix

$$\begin{bmatrix} 0 & -a_3 & a_2 \\ a_3 & 0 & -a_1 \\ -a_2 & a_1 & 0 \end{bmatrix}$$

where $A = [\, a_1 \; a_2 \; a_3 \,]^T$

B = transformation matrix relating Euler rates to body rates
$C1,C2,C3$ = the cosine of φ_1, φ_2 and φ_3, respectively
D = the state canonical equation disturbance matrix
E_3 = the 3×3 unit matrix
G_1,G_2 = roll channel rate and attitude acceleration gains (rad/sec, rad/sec^2)
G_3,G_4 = pitch channel rate and attitude acceleration gains (rad/sec, rad/sec^2)
G_5 = yaw to roll coupling gain
G_H = adaptive gain
ΔG_H = incremental adaptive gain correction
H_n = nominal wheel momentum along the $-Y$-axis (ft-lb-sec)
h = DGW angular momentum vector (ft-lb-sec)
Δh_E = momentum error (ft-lb-sec)
h_W = the instantaneous wheel momentum magnitude (ft-lb-sec)
h_{wc} = the instantaneous wheel momentum rate magnitude (ft-lb)
I = vehicle inertia tensor (slug-ft^2)
I_E = estimated vehicle inertia tensor (slug-ft^2)
M_D = disturbance torque (ft-lb)
R_T = adaptive gain parameter
$S1,S2,S3$ = the sine of φ_1, φ_2 and φ_3, respectively
T_s = sample interval (sec)
$t\varphi_i$ = the tangent of φ_i
U, $\dot{U}$ = the geocentric orbit rate and acceleration (rad/sec, rad/sec^2)
X,Y,Z = the vehicle body axes
Z^{-1} = the z transform of a sample delay
δ = differential operator
ξ_x,ξ_y,ξ_z = roll, pitch and yaw damping ratio, respectively
$\varphi_1,\varphi_2,\varphi_3$ = yaw, roll and pitch Euler angles (rad)
$\ddot{\varphi},\dot{\varphi},\varphi$ = $[\ddot{\varphi}_1 \; \ddot{\varphi}_2 \; \ddot{\varphi}_3]^T$, $[\dot{\varphi}_1 \; \dot{\varphi}_2 \; \dot{\varphi}_3]^T$, $[\varphi_1 \; \varphi_2 \; \varphi_3]^T$, (rad/sec^2, rad/sec, rad)
$[\varphi_i]_j$ = direction cosine matrix defining the ith rotation about the jth axis
ω = vehicle angular velocity (rad/sec)
$\dot{\omega}_c$ = control law acceleration (rad/sec^2)
$\dot{\omega}$ = vehicle angular acceleration (rad/sec^2)
$\omega_{nx},\omega_{nx},\omega_{nz}$ = roll, pitch and yaw undamped natural frequencies (rad/sec)
ω_o = orbit angular velocity vector (rad/sec)
$\dot{\omega}_o$ = orbit angular acceleration vector (rad/sec^2)

Subscripts and Superscripts

$()_C$ = the C subscript denotes the commanded values
$(.)'$ = the prime superscript denotes the model variables
$(\,)_,$ = the vector time derivative with respect to body frame

Introduction

A STUDY was initiated to develop a digital controller for the attitude maneuvering of a satellite using a momentum biased double gimballed reaction wheel (DGW)[1] as the actuating mechanism. It was assumed that the maneuvering controller would be used on board a long-life synchronous satellite equipped only with a roll and pitch horizon sensor. Reliability and complexity considerations prohibited the use of yaw sensor. Figure 1 shows a simplified sketch of the relative orientation of the DGW and the horizon sensor with respect to the vehicle control axes.

Presented as Paper 74-898 at the AIAA Mechanics and Control of Flight Conference, Anaheim, California, August 5-9, 1974; submitted August 26, 1974; revision received February 20, 1975.
Index category: Spacecraft Attitude Dynamics and Control.
*Staff Engineer, Guidance and Control Systems. Member AIAA.
†Research Engineer, Guidance and Control Systems. Member AIAA.

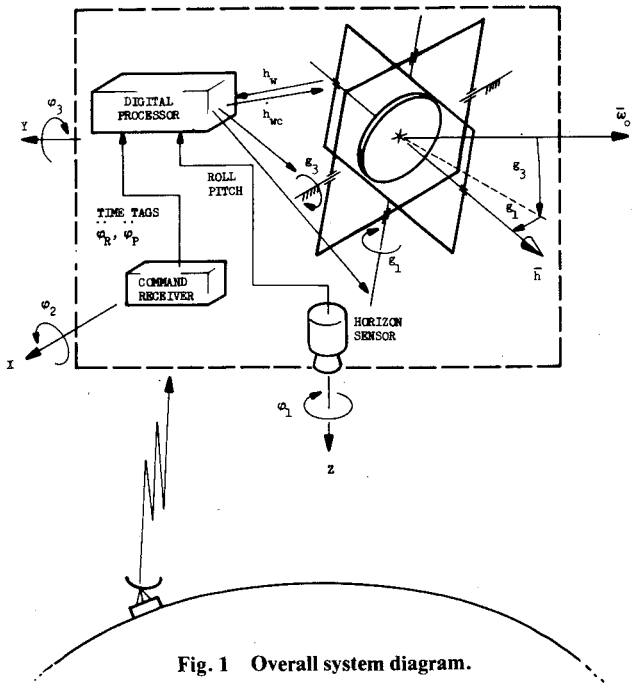

Fig. 1 Overall system diagram.

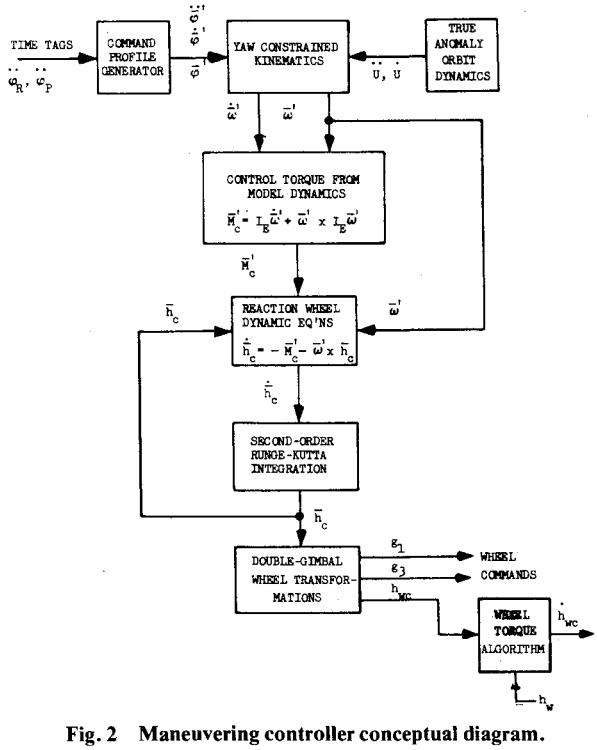

Fig. 2 Maneuvering controller conceptual diagram.

The basic design goals for the maneuvering controller were the following. a) Large-angle maneuvering capability. The maneuvering controller would have to be capable of $\pm 10°$ roll and/or pitch maneuvers. b) Precise maneuvered angle capability. The maneuvered angles would have to be within $\pm 0.01°$ of the commanded angles. c) Rapid maneuvering capability. The maneuvering times would have to be small compared to the attitude-hold control system time constants. d) Serial maneuvering capability. The maneuvering controller would have to be capable of serial maneuvers with no intervening settling time.

The lack of yaw information restricted these capabilities to roll and pitch maneuvering, and also necessitated that the long time constant yaw axis not be excited. Yaw has a long time constant because yaw attitude stabilization depends on gyroscopic wheel stiffness and a roll actuated yaw torque (WHECON-type system).[2] For the vehicle parameters used in the study, any significant yaw angle or rate at the end of a maneuver would require 5000 sec before the yaw attitude reached its steady-state value. This was undesirable because of quick serial maneuvers would not be possible.

The initial concept was to use a special maneuvering controller, and revert to a digital version of the DGW controller described in Ref. 3 to stabilize the vehicle about the maneuvered attitude upon maneuver termination. However, during the course of the analysis it became apparent that the maneuvering controller, with slight modifications, could also be used to control the vehicle during normal attitude-hold operation. The capability of having both maneuvering and attitude control in one system was highly desirable since it would minimize the complexity of the overall control system. Hence, the study objective became to develop a single dual mode controller.

This paper then is concerned with the development of a single controller, which with simple modifications, could be switched to either a rapid, large-angle maneuvering controller or a normal attitude-hold controller capable of stabilizing the vehicle about the maneuvered attitude. Such a controller would allow a communications satellite to spot beam to locations anywhere on the earth. Also, any orbit eventually drifts and maneuvering the vehicle attitude could reduce the number of orbit adjustments required during a mission. The ability to make serial, rapid and precise large angle maneuvers would greatly enhance the effectiveness of an Earth Resources Technology Satellite (ERTS).

The controller is a digital processor which simulates a model of the vehicle/wheel system with the yaw angle constrained to zero. In the maneuvering mode, the controller operates open loop to avoid the long time constants associated with the DGW control system. During a maneuver the processor inputs are the monitored wheel momentum and the roll/pitch maneuver profile. The profiles are defined by the roll and pitch accelerations and the time tags associated with their common acceleration, coast, and deceleration segments. Given the latter inputs, the processor's command profile generator calculates the time history of the Euler angle, rate and accelerations defining the slew. Given the Euler angle, rate, and accelerations, the processor generates the estimated angular velocity and acceleration of the vehicle and forms the inertial reaction torque profile to realize the maneuver. Using Euler's equation and Coriolis's law, the processor transforms the inertial reaction torque profile to a vehicle coordinated time rate of change of angular momentum profile which is then integrated to obtain the wheel angular momentum needed for the given maneuver. For noncircular orbits, the true anomaly equation must be programed in the processor to provide the values of the geocentric rate and acceleration needed for the angular velocity and acceleration. The calculated wheel momentums are then transformed to gimbal angles and wheel momentum along the wheel spin axis. The wheel momentum command and monitored wheel momentum are fed into a wheel torque algorithm which outputs an adjusted wheel torque command that compensates for any deviation from the expected wheel torque gain. Figure 2 shows a conceptual diagram of the maneuvering controller.

In the attitude-hold mode, the commanded angles and rates are replaced by the vehicle's actual roll/pitch angles and rates, and the commanded accelerations are set to zero. The vehicle's actual angles and rates are obtained by transforming the filtered horizon sensor signals to an Euler angle set with subsequent differentiation. These are input to the processor to decouple the axes except for yaw into roll. Attitude control is obtained by summing the commanded vehicle angular acceleration with the processor's calculated angular acceleration obtained with the new inputs. The commanded body acceleration is formed by a control law which uses linear combinations of the vehicle's roll/pitch angles and rates. The only

other change to the processor in the attitude-hold mode is that the gain compensation portion of the wheel torque algorithm is inoperative. Figure 3 is a conceptual diagram of the attitude-hold controller.

The attitude-hold controller operates in essentially the same way as the DGW controller described in Refs. 1 and 3. In fact, for control about nadir the equations describing the vehicle behavior are identical. However, the yaw-to-roll gain ratio, used in the yaw control law, varies for the attitude controller presented in this paper. The yaw-to-roll gain ratio must vary as a function of the vehicle attitude and wheel momentums in order to maintain a constant yaw damping ratio.

Simulation results are presented which demonstrate that the controller is capable of any maneuver within hardware limitations, and of performing serial maneuvers with no intervening settling time. The results show that the maneuvers are executed with near-zero yaw angle and rate.

Analysis and simulation results are presented which demonstrate the stability of the attitude controller about any vehicle attitude. Linear analysis conducted with a computer program to assess the effects of factors intractable by hand analysis (i.e., orbit eccentricity, cross products of inertia, model inertia tensor errors, and hardware misalignments) is described, and the results summarized. Results of a full-scale nonlinear simulation used to verify the linear analysis and to assess the effects of nonlinearities, such as quantization and vehicle kinematics and dynamics, are also presented.

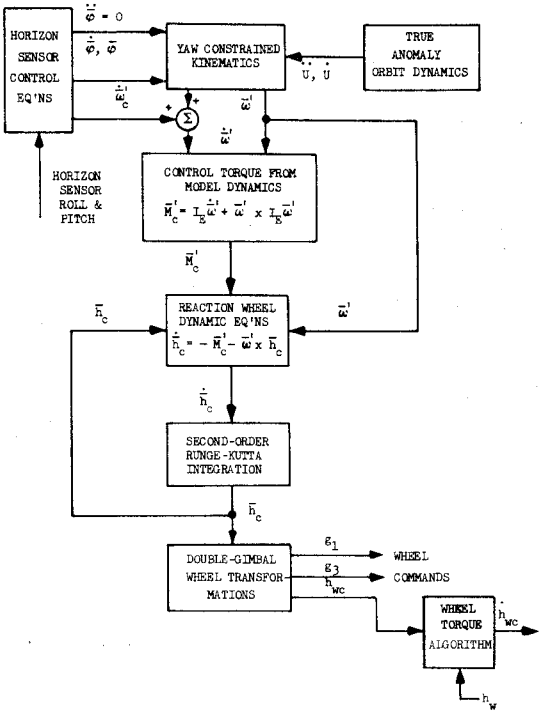

Fig. 3 Attitude-hold controller conceptual diagram.

System Equations—Maneuvering Mode

The vehicle/wheel system equations and the maneuvering mode model equations are:

$$\omega' = [\varphi_3']_2 V \tag{1}$$

$$\dot{\omega}' = [\varphi_3']_2 A \tag{2}$$

$$\dot{h}_c = -I_E\dot{\omega}' - \omega' \times I_E\omega' - \omega' \times h_c \tag{3}$$

$$h_c = \int_0^t h_c dt \tag{4}$$

$$\omega = B\dot{\varphi} + T\omega_0 \tag{5}$$

$$\dot{\omega} = I^{-1}(M_D - \omega \times I\omega - \dot{h} - \omega \times h) \tag{6}$$

$$\ddot{\varphi} = B^{-1}(\dot{\omega} - CR + \omega \times T\omega_0 - T\dot{\omega}_0) \tag{7}$$

where

$$V = [\dot{\varphi}_2', \dot{\varphi}_3', -\dot{U}C_2', \dot{U}S_2']^T \tag{8}$$

$$A = \begin{bmatrix} \ddot{\varphi}_2' - \dot{U}\dot{\varphi}_3' S2' \\ \ddot{\varphi}_3' - \ddot{U}C2' + \dot{U}\dot{\varphi}_2' S2' \\ \dot{\varphi}_2'\dot{\varphi}_3' + \ddot{U}S2' + \dot{U}\dot{\varphi}_2' C2' \end{bmatrix} \tag{9}$$

$$R = [\dot{\varphi}_2\dot{\varphi}_3, -\dot{\varphi}_1\dot{\varphi}_3, \dot{\varphi}_1\dot{\varphi}_2]^T \tag{10}$$

and

$$B = \begin{bmatrix} -C2S3 & C3 & 0 \\ S2 & 0 & 1 \\ C2C3 & S3 & 0 \end{bmatrix}, C = \begin{bmatrix} -S3 & C2C3 & S2S3 \\ 0 & 0 & C2 \\ C3 & C2S3 & -S2C3 \end{bmatrix} \tag{11}$$

Prime superscripts are used to differentiate the model variables from the actual vehicle variables. The model values for the geocentric rate and acceleration are not differentiated from the actual values because these variables are assumed to be known with a great deal of accuracy. In deriving the above equations the following conventions were used: The orbit x-axis is in the direction of flight, the orbit y- axis is normal to the orbit plane opposite to the orbit rate vector, and the orbit z-axis is directed toward the earth along the earth to satellite radius vector. The satellite control axes are related to the orbit axes by a 312 Euler angle set. Hence, the transformation matrix from the orbit axes to the vehicle axes is

$$T = [\varphi_3]_2\,[\varphi_2]_1\,[\varphi_1]_3$$

Maneuvering Controller

The maneuvering controller is basically obtained by simulating Eqs. (1-7) in a digital processor. However, the processor must also include ancillary algorithms needed to make the controller compatible with the commands required to actuate the DGW, and to tailor the controller to the particular vehicle orbit. The latter requirement may be seen by noting that for a noncircular orbit a true anomaly algorithm is required to generate $\ddot{U}$ in order to calculate the correct desired angular acceleration. The DGW was designed to accept time rate of change of momentum and gimbal angle commands; hence the processor must incorporate an integration algorithm to obtain h_C and subsequent algorithms to transform the h_C command to the proper commands. The transformation is done in two stages. The h_C command is first transformed to the required gimbal angle commands, and to a wheel momentum command. Secondly, the wheel momentum command plus the monitored wheel momentum are input to a wheel torque algorithm where they are used to generate a time rate of change of momentum command. The wheel torque algorithm includes an adaptive gain algorithm which automatically adjusts the wheel momentum rate command to compensate for any deviation in the actual wheel torque gain. The adaptive gain is required because any error in the hardware gain would result in erroneous maneuvers. The DGW was designed to accept torque commands rather than momentum command in order to improve commanded signal

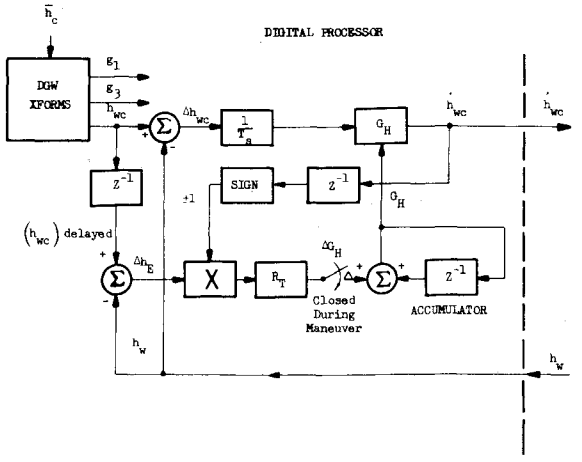

Fig. 4 Wheel torque algorithm block diagram.

resolution limited by D to A converters, and eliminate the rather long time constant associated with the wheel momentum control loop. This technique was chosen to ensure accurate maneuvers.

Figure 2 is a conceptual diagram of the maneuvering controller. A maneuver is executed by relaying the defining parameters of the roll and pitch accelerations to the command profile generator. The defining parameters are the roll and pitch accelerations ($\ddot{\varphi}_R$, $\ddot{\varphi}_R$), and the common time tags associated with their acceleration, coast, and deceleration segments. At each sample instant, the following functions are then performed. The command profile generator calculates the Euler angle, rate, and acceleration profiles, and transfers them to the yaw constrained kinematics block. Here, the Euler profiles are used to calculate the model angular velocity and acceleration values. The next block computes the model torque which is subsequently transformed by the reaction wheel dynamics equation's block to the time rate of change of wheel momentum command, $\dot{h}_C$. Next, the integration block calculates the angular momentum of the wheel,$\boldsymbol{h}_C$. The $\boldsymbol{h}_C$ command is finally transformed to the controller's outputs: the compensated wheel torque command, $\dot{h}_{wc}$, and the gimbal angle commands, g_1 and g_3. This is done via the DGW transformations block and the wheel torque block. It should be noted that because of the sampled nature of the controller the commands lead the wheel's actual momentum and gimbal angles by one sample interval. In other words, the controller's commands may be thought of as future commands.

The DGW transformations block is comprised of equations which transform the computed wheel momentum components to a wheel momentum command along the spin axis, and to gimbal angle commands. The transformation equations are based on a $-1, 3$ rotational sequence. This sequence was used to conform to the mechanization of the wheel gimbal movements.

Figure 4 shows a block diagram representation of the wheel torque algorithm. The h_{wc} input to the algorithm is the value desired by the next sample instant. This momentum will be obtained by forming a torque command equal to the Δh_{wc} command (difference between the future command value h_{wc}, and the present measured wheel momentum, h_w) divided by the sample interval.

The adaptive gain algorithm forms a gain, G_H, by adding ΔG_H values to the gain's nominal value. The ΔG_H are formed by first comparing the present value of the command wheel momentum against the present value of the measured wheel momentum. Their differences, Δh_E, is corrected for sign and multiplied by the parameter R_T to finally obtain ΔG_H. When the measured wheel momentum exactly equals the commanded value the gain G_H no longer changes and exactly compensates for any error in the actual wheel torque gain. The parameter R_T is set to a value 0.1. The approximate time constant of the adaptive gain algorithm is T_S/R_T or 100 sec in this case.

Attitude-Hold Controller Linear Analysis

Using the definitions of reference axes and their relationships as set forth previously, the vehicle wheel/system in the attitude-hold mode is completely described by Eqs. (1) and (3-7). Equation (2) becomes

$$\dot{\omega}' = [\varphi_3']_2 A + \dot{\omega}_c' \tag{12}$$

where now

$$A = \begin{bmatrix} -\ddot{U}\phi_3' S2' \\ -\ddot{U}C2' + \dot{U}\dot{\phi}_2' S2' \\ \dot{\phi}_2'\dot{\phi}_3' + \dot{U}S2' + \dot{U}\dot{\phi}_2' C2' \end{bmatrix} \tag{13}$$

and

$$\dot{\omega}_c' = \begin{bmatrix} -G_1\dot{\varphi}_2' - G_2(\varphi_2' - \varphi_{2B}) \\ -G_3\dot{\varphi}_3' - G_4(\varphi_3' - \varphi_{3B}) \\ -G_5\{-G_1\dot{\varphi}_2' - G_2(\varphi_2' - \varphi_{2B})\} \end{bmatrix} \tag{14}$$

The states of the vehicle/wheel system were chosen to be $\dot{\varphi}$, φ, and $\boldsymbol{h}$. Assuming that the model Euler variables were exactly equal to the actual Euler variables, and that $\boldsymbol{h}_c \equiv \boldsymbol{h}$ the system equations were linearized about any general vehicle roll/pitch offset, and put into the state canonical form expressed by Eq. (15).

$$\begin{bmatrix} \ddot{\varphi} \\ \dot{\varphi} \\ \dot{\boldsymbol{h}} \end{bmatrix} = \begin{bmatrix} F_1 & F_2 & F_3 \\ E_3 & 0 & 0 \\ F_4 & F_5 & F_6 \end{bmatrix} \begin{bmatrix} \dot{\varphi} \\ \varphi \\ \boldsymbol{h} \end{bmatrix} + DU \tag{15}$$

the partitioned matrices F_1 through F_6 are equal to

$$F_1 = \frac{\partial \ddot{\varphi}}{\partial \dot{\varphi}} \quad F_2 = \frac{\partial \ddot{\varphi}}{\partial \varphi} \quad F_3 = \frac{\partial \ddot{\varphi}}{\partial \boldsymbol{h}} \tag{16}$$

$$F_4 = \frac{\partial \dot{\boldsymbol{h}}}{\partial \dot{\varphi}} \quad F_5 = \frac{\partial \dot{\boldsymbol{h}}}{\partial \varphi} \quad F_6 = \frac{\partial \dot{\boldsymbol{h}}}{\partial \boldsymbol{h}} \tag{17}$$

The most general expression for F_3 is

$$F_3 = B^{-1} I^{-1} [(\omega' - \omega) x] \tag{18}$$

Since F_3 is evaluated for an orientation where the yaw angle is approximately zero, $\omega' \cong \omega$ and thus $F_3 \cong 0$. Therefore, the vehicle behavior can be studied independently of the wheel behavior by evaluating F_1 and F_2.

About nadir, the expressions for F_1 and F_2 reduce to the equations found in Ref. 3. This is detailed in Ref. 4. The values of G_1 through G_5 were chosen by using the linearized nadir equations.

To evaluate the effectiveness of the gains chosen when the vehicle is offset in some general roll/pitch offset is quite difficult because of the complexity of the expressions for F_1 and F_2. To evaluate the stability of the system when products of inertia are included, when the model inertias differ from the actual vehicle inertias, or when orbit eccentricity is included,

Table 1 Vehicle roots for various attitudes and wheel momentums

					Ideal Conditions[a]		
Vehicle angle (deg)		Roll		Pitch		Yaw	
φ_2	φ_3	ω_{nx}	ξ_x	ω_{ny}	ξ_y	ω_{nz}	ξ_z
0	0[b]	0.020	0.670	0.020	0.707	0.0010	0.701
30	30[c]	0.023	0.855	0.020	0.707	0.0011	0.712
−30	−30	0.032	1.039	0.020	0.707	0.0010	0.645
					Nonideal conditions		
φ_2	φ_3	ω_{nx}	ξ_x	ω_{ny}	ξ_y	ω_{nz}	ξ_z
0	0[b]	0.021	0.752	0.020	0.700	0.0010	0.455
30	30[c]	0.024	0.894	0.021	0.742	0.0011	0.623
−30	−30	0.034	1.094	0.021	0.744	0.0010	0.902

[a] Ideal conditions: no hardware misalignments, $I_E = I$. [b] Nadir conditions: $h = [0 \quad -30 \quad 0]^T$; eccentricity = 0. [c] Large-angle offset: $h = [-13 \quad -23 \quad 13]^T$; eccentricity = 0.2.

is impossible because the derivation alone of the F_1 and F_2 matrices becomes intractable. This problem was circumvented by using a computer program, referred to as the root program, to calculate the partitioned F matrices. The partitioned matrices were calculated by the numerical equivalent of the definitions of the partitioned matrices. For example, F_1 was calculated in the following way.

$$F_1 \triangleq \frac{\partial \ddot{\varphi}}{\partial \dot{\varphi}} \cong \frac{\ddot{\varphi}\{\dot{\varphi}+\delta\dot{\varphi}, \varphi, h\} - \ddot{\varphi}\{\dot{\varphi}-\delta\dot{\varphi}, \varphi, h\}}{2\delta\dot{\varphi}} \tag{19}$$

With the computer program the partials could be evaluated by operating on the complete equations describing the system. Hence, by incorporating the ability to find the system roots and the steady state vehicle response, the system characteristics could be evaluated for any possible case. For example, the effects of orbit eccentricity, hardware misalignments, etc., could easily be evaluated by use of the root system.

Numerous runs were made with the root program to determine the stability of the system for various roll/pitch offsets and various wheel momenta under ideal conditions (i.e., circular orbit, no products of inertia and the model inertia tensor equal to the actual inertia tensor). It was determined that while the roll/pitch roots were relatively insensitive to the vehicle attitude and the wheel momentum components, the yaw roots changed significantly and could, in fact, move into the right-half root locus plane.

G_5 was the cause of the instability. For large vehicle offsets, the gain value calculated for nadir conditions caused the roll-activated yaw torque to act in the wrong direction. This problem was corrected by finding the G_5 functional relationship required to maintain a constant yaw damping ratio. It was found that G_5 varies as a function of the wheel momentum and the vehicles roll/pitch attitude.[4]

Linear Analysis Results

The control gains were chosen to be compatible with the hardware quantization characteristics, the control system sample interval and to result in the following natural frequencies and damping ratios:

$$\omega_{nx} = 0.02 \text{ rad/sec} \qquad \xi_x = 0.707$$

$$\omega_{ny} = 0.02 \text{ rad/sec} \qquad \xi_y = 0.707$$

$$\omega_{nz} = 0.001 \text{ rad/sec} \qquad \xi_z = 0.707$$

Using the appropriate gains, the root program was used to determine the vehicle stability over a wide range of roll and/or pitch offset attitudes and initial wheel momentum components for the following conditions. It was assumed that no hardware misalignments existed, the horizon sensor had no bias associated with it, the model inertia tensor was equal to the actual inertia tensor and the orbit was circular. It was found that the roll, pitch, and yaw roots were insignificantly affected for any allowable initial wheel momentum components and for any roll/pitch offsets within ±20°. At vehicle offsets of ±30° the roll roots become negative real, while the pitch and yaw roots continued to show insignificant change. An orbit eccentricty of 0.2 did not alter the previous results. Hence, the attitude-hold control system is capable of stabilizing an eccentric orbit vehicle about offsets at least equal to ±30° in roll and/or pitch.

The effect of nonideal conditions (that is hardware misalignments, horizon sensor bias error, the model inertia tensor different from the vehicle inertia tensor and orbit eccentricity) was also evaluated. The misalignments were taken to be 1.0° in roll, pitch, and yaw for both the horizon sensor and wheel; the horizon sensor bias was taken to be 1.0° in both roll and pitch. The model inertias were assumed to be 10% higher than the actual inertias, and the model products of inertia were assumed to be 100 slug-ft^2 while the vehicle had zero products of inertia. These nonideal conditions do not reflect expected discrepancies, but are exaggerated values used to assess their affect on the system stability. It was found that the yaw damping ratio changed from 0.707 to 0.5 under the worst nonideal conditions.

Table 1 shows the vehicle roots about nadir for ideal conditions and for nonideal conditions input simultaneously. It also gives the roots of the system for attitude-hold about roll/pitch offsets equal to ±30° with an orbit eccentricity of 0.2 and the nonideal conditions input simultaneously. The effect of the nonideal conditions and external body torques on the vehicle's steady-state response was also determined using the root program. The results of these runs agree with those obtained using the misalignment equations in Ref. 3.

Full-Scale Digital Simulation

A full-scale nonlinear simulation was written to verify the results of the linear analysis, to assess the effects of the discrete nature of the controller, and to assess the effect of the hardware characteristics on vehicle performance. In the simulation the sample interval was set to 10 seconds, and it was assumed that the wheel actuating controls would have infinite bandwidth. Table 2 summarizes the system parameters used in the simulation.

Maneuvering Simulation Results

Figure 5 shows the vehicle's angle and rate response during a maneuver made when the vehicle was offset 6.0° in roll and pitch. The maneuver is defined in Table 3.

The length of the execute times were dictated by the maximum torque capability of the wheel, 0.05 ft-lb. Figure 5c

shows that the maximum yaw angle obtained during the maneuver was about 0.004° while Fig. 5f indicates the maximum yaw rate was about 0.00008°/sec. In fact, these were the upper bounds of the yaw angle and rate for the entire run, which was much longer than the 1000 seconds as shown in Fig. 5. The run was made assuming only gravity gradients torques acting on the vehicle.

Computer runs were also made to verify the controller's ability to maneuver to extreme angles. For example, a −32.0° simultaneous roll and pitch maneuver was simulated. For this run the horizon sensor saturation limits were set to ±35°. Even for this extreme maneuver the maximum yaw angle excursion was 0.23°. The maximum yaw rate was found to be 0.0003°/sec. The run was made assuming only gravity gradient torques acting on the vehicle.

Runs were also made assuming disturbance torques on the order of 1×10^{-4} ft-lb. The maneuvering capability of the controller was unaffected.

Table 4 shows how individual nonideal conditions affect the ability of the maneuvering controller. Table 4 may be summarized by the following observations: I_{EI} error causes

Table 2 System parameters

I_1 = 3582 ft-lb-sec^2	G_1 = 0.02828 rad/sec
I_2 = 1730	G_2 = 0.0004 rad/sec^2
I_3 = 2200	G_3 = 0.02828 rad/sec
$I_{12} = I_{23} = I_{31} = 0$	G_4 = 0.0004 rad/sec^2
$\omega_o = 0.7292^{-4}$ rad/sec	
eccentricity = 0.2	
Horizon sensor	**Digital processor**
Quant = 0.004°	General-purpose computer
Saturation = 12°	
Smoothing time = 10 sec	Computation interval = 10 sec
Double gimbal wheel	
Angular momentum limits	= 24-36 ft-lb-sec
Angular momentum readout quant	= 0.0004 ft-lb-sec
Wheel torque quant	= 0.0001 ft-lb
Wheel torque limits	= 0.05 ft-lb
Gimbal angle quant	= 0.01°
Gimbal angle limits	= 30°
Maximum gimbal angle rate	= 1°/sec

Table 3 Profile history

Maneuver	Maneuver times (sec)
2.4° roll and pitch	0-170
0.1° roll	170-200
−0.1° roll	200-230
0.1° pitch	230-260
−0.1° pitch	260-290
Arbitrary roll, pitch maneuver	290-320

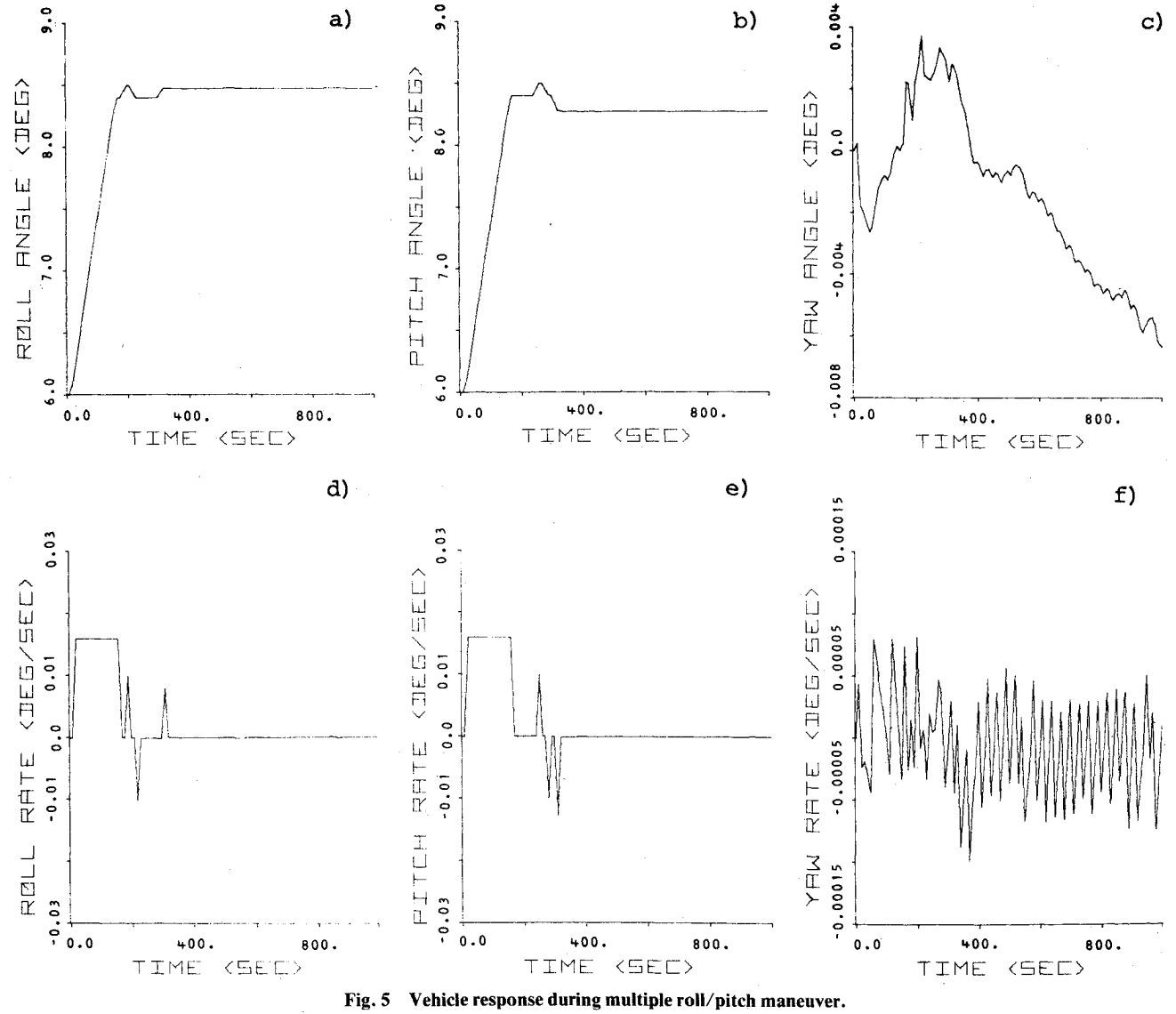

Fig. 5 Vehicle response during multiple roll/pitch maneuver.

Table 4 2.4° roll and pitch maneuver from 6.0° initial roll/pitch offset[a]

Case run	φ_1 (°/sec)	φ_1 (deg)	$\dot{\varphi}_2$	φ_2	$\dot{\varphi}_3$	φ_3
Everything exact	0.0	0.00214	0.00003	8.39900	0.00006	8.40144
$I_{E1} = 1.1\ I_1$	0.00211	0.18747	−0.00145	8.56446	0.00001	8.38504
$I_{E2} = 1.1\ I_2$	−0.00006	−0.00547	−0.00005	8.39877	0.00166	8.63400
$I_{E3} = 1.1\ I_3$	−0.00019	0.02403	−0.00022	8.38588	0.00008	8.39856
$I_{E13} = 100$	−0.00063	0.07824	−0.00069	8.35686	0.00009	8.39063
$I_{E23} = 100$	−0.00074	0.07295	−0.00066	8.34932	0.00026	8.41049
$I_{E12} = 100$	0.00054	0.04993	−0.00044	8.44416	0.00097	8.53015
DGW yaw[b] = 1°	0.00010	0.01174	−0.00009	8.37591	0.00005	8.48594
DGW roll = 1°	0.00002	0.03370	−0.00004	8.40113	0.00006	8.39038
DGW pitch = 1°	0.00015	−0.05980	0.00014	8.40936	0.00004	8.40934
H/S roll bias = 1°	0.00008	0.00740	0.00002	8.40609	0.00005	8.40072
H/S pitch bias = 1°	0.00007	0.04661	−0.00005	8.40020	0.00005	8.39577
H/S yaw = 1°	0.00003	−0.00103	0.0	8.40106	0.00006	8.40183
H/S roll = 1°	0.00008	0.00872	0.00001	8.40582	0.00005	8.40059
H/S pitch = 1°	0.00007	0.04661	−0.00005	8.40020	0.00005	8.39577

[a] Results are at maneuver termination. [b] Misalignment error.

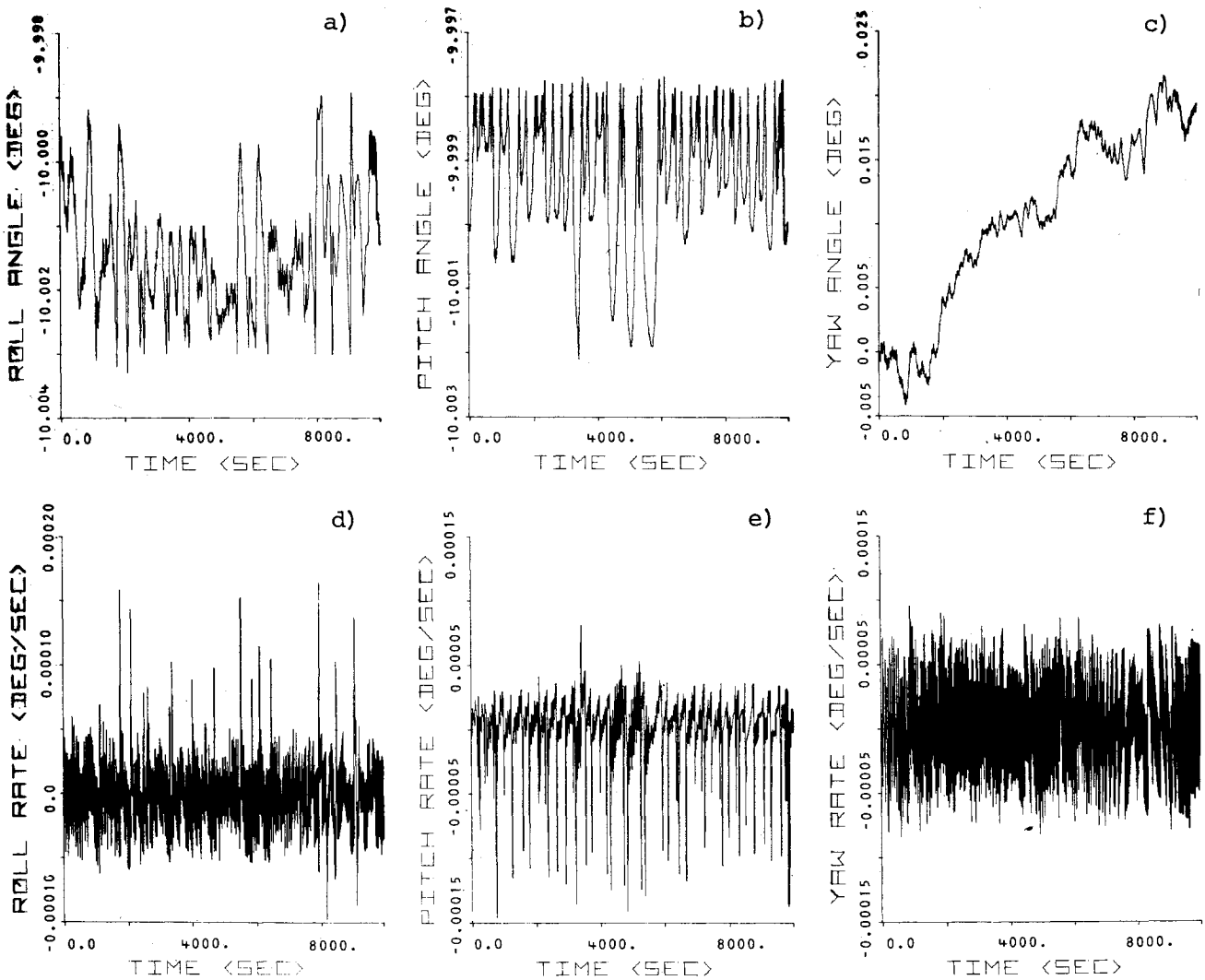

Fig. 6 Vehicle attitude-hold response about −10° roll and pitch offset.

roll and yaw error, I_{E2} error causes pitch error, I_{E13} error causes roll and yaw error, I_{E23} error causes roll and yaw error, I_{E12} error causes pitch and yaw error, and yaw gimbal misalignment causes pitch error.

Attitude-Hold Simulation Results

Figure 6 shows the vehicle response to attitude hold about −10° in roll and pitch. Only gravity gradient disturbance torques were acting; the yaw response is due to the gravity gradient torques. The figure shows that the attitude-hold accuracy is dominated by the granularity of the smoothed horizon sensor signals. The peak rate spikes in the roll and pitch rate responses are proportional to the smoothed horizon sensor quantization level divided by the sample interval.

From numerous runs, the following attitude-hold controller characteristics were also observed: 1) The steady-state yaw attitude error is approximately equal to a DGW yaw alignment error. 2) The steady-state roll attitude error is approximately equal to a horizon sensor roll bias error or a horizon sensor roll misalignment error. This observation is also true for pitch

attitude errors. 3) Model inertia deviation from the actual vehicle inertia has insignificant effect on attitude control.

Conclusions

The controller is capable of precise large-angle maneuvers and of stabilizing the vehicle about the maneuvered attitude. The limitations on the controller's capability are imposed only by hardware constraints. Roll and/or pitch maneuvers may be performed serially without any intervening settling time, and without exciting the yaw axis. The controller is capable of accurate attitude control of a satellite in eccentric orbit. The attitude-hold accuracy is dominated by the granularity of the smoothed horizon sensor signals. The controller has the growth potential of an active independent yaw channel.

References

[1] Scott, E.D., "Double-Gimballed Reaction Wheel Control System," First Western Space Conference, Santa Maria, Calif., Oct. 1970.

[2] Dougherty, H.J., Scott, E.D., and Rodden, J.J., "Analysis and Design of WHECON—An Attitude Control Concept," AIAA Paper 68-461, San Francisco, Calif., 1968.

[3] Lyons, M.G., et al., "Double Gimballed Reaction Wheel Attitude Control System for High Altitude Communications Satellites," AIAA Paper 71-949, Hempstead, N.Y., 1971.

[4] Scott, E.D., and Rubbo, J.E., "Double Gimballed Reaction Wheel Maneuvering and Attitude Control System," AIAA Paper 74-898, Anaheim, Calif., 1974.